İmalat Teknolojileri ve Uygulamaları
Cilt: 3, No: 3, 2020 (20-30)
Araştırma Makalesi
e-ISSN: 2717-7475

Manufacturing Technologies and Applications
Vol: 3, Issue: 3, 2020 (20-30)
Research Article
e-ISSN: 2717-7475

Optimization of Welding Parameters in MAG Lap Welding of DD13 Sheet Metal with Taguchi Method and FEM Analysis

Serkan APAY[1]

[1] *Düzce Üniversitesi, Mühendislik Fakültesi, Düzce, Türkiye*

ARTICLE INFORMATION

Received: *17.10.2022*
Accepted: *13.11.2022*

Keywords:
Finite element analysis
Hardness
Heat input
MAG welding
Taguchi method

ABSTRACT

In this study, DD13 sheet materials used in automobile swing manufacturing were welded with GMAW (Gas Metal Arc Welding) welding method with different parameters such as welding method, welding amperage, and welding speed. The optimized value of the welding parameters, which will give the lowest hardness value in the weld seam hardness, was calculated by the Taguchi method. In addition, the heat input values that are thought to affect the hardness change were calculated, and the results were used to interpret the hardness change and Taguchi optimization values. After the experimental studies, the optimized value was compared with the actual results, and the verification test was performed. As a result of the optimization process, the lowest hardness value was estimated as 172.98 HV0.1 in MAG welding performed at 420 min/mm welding speed, 290 A, and 33.6 V parameters. The validation test result was found to be consistent with 173.4 HV0.1. Based on these values, finite element analysis (FEM) was performed with Simufact Welding 8.0 software. As a result of the investigation, the weld macrostructure, thermal changes, and the amount of distortion were examined. The results obtained are in agreement with the validation experiments.

Taguchi Metodu ve FEM Analizi ile DD13 Sacların MAG Bindirme Kaynağında Kaynak Parametrelerinin Optimizasyonu

MAKALE BİLGİSİ

Alınma: *17.10.2022*
Kabul: *13.11.2022*

Anahtar Kelimeler:
Sonlu elemanlar analizi
Sertlik
Isı girdisi
MAG kaynağı
Taguchi metodu

ÖZET

Bu çalışmada, otomobil salıncak imalatında kullanılan DD13 sac malzemelerinin GMAW (Gas Metal Arc Welding) kaynak yöntemi ile kaynak yöntemi, kaynak amperi ve kaynak hızı gibi farklı parametreler ile kaynatılmıştır. Kaynak parametrelerinin, kaynak dikişi sertliğinde en düşük sertlik değerini verecek optimize değer Taguchi yöntemiyle hesaplanmıştır. Ayrıca sertlik değişimine etkisi olduğu düşünülen ısı girdisi değerleri hesaplanmış, çıkan sonuçlar sertlik değişimi ve Taguchi optimizasyonu değerlerini yorumlamada kullanılmıştır. Yapılan deneysel çalışmalardan sonra çıkan optimize değer gerçek sonuçlar ile karşılaştırılmış ve doğrulama testi yapılmıştır. Optimize işlemi sonucunda en düşük sertlik değeri tahmini 172.98 HV0.1 olarak 420 min/mm kaynak hızında, 290 A ve 33.6 V parametreleri ile yapılan MAG kaynağında ulaşılmıştır. Doğrulama testi sonucu 173.4 HV0.1 ile tutarlı olduğu görülmüştür. Sonlu elemanlar analizi (FEM) bu değerler temel alınarak Simufact Welding 8.0 yazılımı ile yapılmıştır. Analiz sonucu kaynak makro yapısı, termal değişimler ve çarpılma miktarı incelenmiştir. Elde edilen sonuçlar doğrulama deneyleri ile yakınlık göstermektedir.

1. INTRODUCTION (GİRİŞ)

Although automobiles today contain many technological innovations, some mechanical components are still used unchanged. One of these components is the swings. Swings have an essential role in the automotive industry [1,2]. Wishbones are vital parts of the vehicle's front

Sorumlu yazar, e-posta: *serkanapay@duzce.edu.tr*
To cite this article: *S. Apay, Optimization of Welding Parameters in MAG Lap Welding of DD13 Sheet Metal with Taguchi Method and FEM Analysis, Manufacturing Technologies and Applications, 3(3), 20-30, 2022.*
https://doi.org/10.52795/mateca.1190277,

suspension, from the classic cars of the past to today's modern vehicles [2,3]. It is the element that connects the swing wheel to the vehicle chassis [4]. There is a wheel at one end of the swing and a chassis [5]. In general, wishbones are produced from medium-carbon and low-carbon steels. These parts have been made from aluminum and similar light metals for fuel economy [6]. Figure 1 shows the swing picture.

Figure 1. Vehicle swing arm (Araç salıncak kolu)

Gas shielded welding methods are preferred as the welding method in most productions made from low carbon and medium carbon steel materials [7,8]. The welded connection method must also be made according to the end-use point where the produced part becomes the final product. Metal microstructures that change after welding can cause problems for long-term working details [9]. Since this problem minimizes welded joints made with the lowest possible heat input, low heat input welding methods are preferred in most joints [10]. Laser, plasma, TIG, and CMT welding are just a few of the low heat input welding methods used today [11–16].

In cases where speed is of great importance in the mass production of parts for the automotive sector, laser welding is not widely used due to the initial setup cost. TIG welding and plasma welding are not widely used due to their slowness. Point resistance welding, MIG-MAG welding, and CMT welding methods, which have faster joints, are frequently used [17–19]. Manufacturing with low heat input welding methods increases the working life of the parts in automobile parts where pulsed work is involved, such as swing manufacturing. With the low heat input generated during welding, the weld seam microstructure is finer-grained and has a faster joining process than the other [20,21]. This situation minimizes the problems that may arise from the welding seam in part.

In this study, welding of DD13 sheets used in swing manufacturing was performed with the MAG welding method at three different volts, three different amperes, and three different welding speeds. The changes in weld seam hardness were examined the results obtained were optimized by the Taguchi method.

2. MATERIAL AND METHOD (MATERYAL VE YÖNTEM)

2.1. Experimental Setup (Deney Düzeneği)

In the experiments, 2.5 mm thick DD13 (EN 10111-2008) sheet metal suitable for cold forming and deep drawing was used. The chemical compositions of the test pieces are given in Table 1, and their mechanical properties are provided in Table 2. 1.2 mm thick ER70S-6 welding wire was used in the welded joint process. The chemical properties of the welding wire are shown in Table 3, and the mechanical properties are shown in Table 4.

Table 1. Chemical composition of DD13 sheet (% by weight) (DD13 saclarının kimyasal bileşimi - % ağırlıkça)

C	Mn	P	S	Si	Al	Cu	Cr	Ni	Mo	Fe
0.04	0.255	0.024	0.001	0.0395	0.053	0.027	0.036	0.035	0.004	Bal.

Table 2. Mechanical properties of DD13 sheet (DD13 saclarının mekanik özellikleri.)

Yield Strength (N/mm^2)	Tensile Strength (N/mm^2)	Elongation (%)
229.5	337.3	42

Table 3. Chemical properties of ER70S-6 welding wire (ER70S-6 kaynak telinin kimyasal özellikleri)

C	Si	Mn	Fe
0.07	0.8	1.45	Bal.

Table 4. Mechanical properties of ER70S-6 welding wire (ER70S-6 kaynak telinin mekanik özellikleri)

Yield Strength (N/mm^2)	Tensile Strength (N/mm^2)	Elongation (%)	Notch Impact Resistance (J) -30°C
460	530	29	50

Welding parameters and the results of these parameters are shown in Table 5. 18 pieces of DD13 sheet materials, 3 mm thick and 100x200 mm in size, were numbered and welded to each other in the form of overlap welding, as shown in Figure 2.

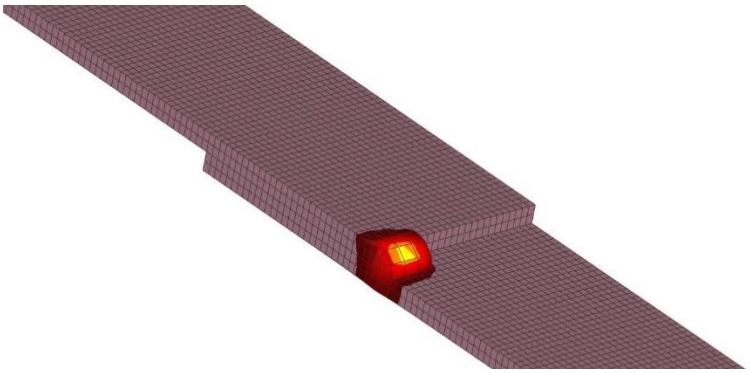

Figure 2. MAG Lap welding schematic (MAG Bindirmeli kaynak şeması)

Table 5. Welding parameters and results for DD13 sheets (DD13 sacları için kaynak parametreleri ve sonuçları.)

Sample No	Welding speed (mm/min)	Amper (A)	Volt (V)	Heat input (KJ/mm)	Hardness result ($HV_{0.1}$)
1	420	250	28	1.0000	177.5
2	420	270	30.2	1.1649	176.2
3	420	290	33.6	1.3920	173.4
4	660	250	30.2	0.6864	183.2
5	660	270	33.6	0.8247	180.6
6	660	290	28	0.7382	181.3
7	900	250	33.6	0.5600	191.7
8	900	270	28	0.5040	194.8
9	900	290	30.2	0.5839	189.7

2.2. Finite Element Modeling

Numerical simulation of the welding process has been one of the crucial topics in welding research for years. Simulation results can explain the physical basis of some unpredictable results in the welding process and optimize welding parameters. However, simulating the welding process is not easy as it involves thermal, mechanical, and metallurgical interactions. Many researchers accept that an essential aspect of the welding process simulation is the correct entry of metallurgical transformations into the model. Correctly entered data has a direct effect on the result.

Finite element analysis of DD13 sheet materials welded in overlapping form with MAG welding method was done with Simufact Welding 8.0 finite element package program. While making the process with a model, it has been ensured that the model is as close to reality as possible by considering the joining method and shape. Modeling and mesh scanning processes were done with

the applications in the same program. The analysis processes examined the microstructure change of the weld zone, the temperature change, and the deformation change. In the analysis process, firstly, the samples were designed as solid models and loaded into the software. The parameters used in the welding process were entered into the software, the materials were loaded into the software, and the analysis process was started.

2.3. Experimental Design and Optimization with Taguchi

Taguchi L9 (3^3) orthogonal array was used for the experimental design; only nine experiments were performed instead of 27 experiments for the full design. It is possible to significantly reduce the number of experiments in the analysis and evaluations made with the Taguchi method. The Taguchi method uses some functions to determine quality characteristics. Since the smallest value is desired in the weld zone hardness measurements, the Taguchi "smallest best" function was used in this study. The selected welding parameters and the levels of these parameters are given in Table 6. The experimental design, experimental results, and signal-to-noise (S/N) ratios calculated according to the experimental results are given in Table 7, considering the L9 orthogonal array.

Table 6. Experiment parameters and levels (Deney parametreleri ve seviyeleri)

Parameters	Level 1	Level 2	Level 3
A Welding Speed (Vw, mm/min)	420	660	900
B Amp (A)	250	270	290
C Volt (V)	28	30.2	33.6

Table 7. Experimental design and experimental results (Deney tasarımı ve deney sonuçları)

Test no	A	B	C	Experimental results and S/N ratios	
	Welding speed (V_W, mm/min)	Amp (A)	Volt (V)	Hardness ($HV_{0.1}$)	S/N_H (dB)
1	420	250	28	177.5	-44.9840
2	420	270	30.2	176.2	-44.9201
3	420	290	33.6	173.4	-44.7810
4	660	250	30.2	183.2	-45.2585
5	660	270	33.6	180.6	-45.1344
6	660	290	28	181.3	-45.1680
7	900	250	33.6	191.7	-45.6524
8	900	270	28	194.8	-45.7918
9	900	290	30.2	189.7	-45.5613

According to the test results, the average value of the hardness results was calculated at 183.156 HV, and the average S/N ratio for the hardness was calculated as -45.25 dB.

2.4. Determining Optimum Levels

In Table 8, the cutting parameters are distinguished by considering the different levels and possible effects of the orthogonal array used in this study. These levels show the average values of the signal-to-noise ratios calculated to analyze the hardness values in the experimental research. These values are used to calculate the estimation values for the determined optimum and random parameters.

Table 8. Averages of S/N ratios (S/N oranlarının ortalamaları)

Welding parameters	Levels			Delta
	Level 1	Level 2	Level 3	
A (Welding speed, V_W)	-44.90	-45.19	-45.67	0.77
B (Amp)	-45.30	-45.28	-45.17	0.13
C (Volt)	-45.31	-45.25	-45.19	0.13

One of the critical steps in the Taguchi method is to determine the optimum levels. Optimum levels are determined by evaluating different levels of experimental parameters, combinations created by the chosen orthogonal array. These levels are used to draw the effect graphs of the levels (Figure 3). When evaluating the main effect graph, the lowest level is considered for these values, as this is the minimum desired stiffness in this study.

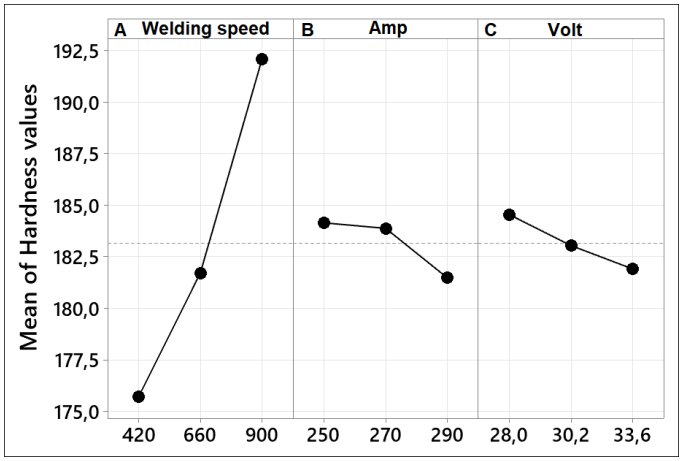

Figure 3. Main effect plot for hardness values (Sertlik değerleri için ana etki grafiği)

According to Figure 3, the optimum combination of test parameters for minimum hardness values was $A_1B_3C_3$ (A_1= 420 mm/min welding speed, B_3 = 290 amp, C_3 = 33.6 Volt).

2.5. Evaluation of Experimental Parameters by Analysis of Variance (ANOVA)

Analysis of variance is used to determine how all control factors used in experimental design affect each other, how this affects performance characteristics, and what changes occur at different levels of the parameters and determine Taguchi confidence intervals [22,23]. The effects of welding speed, amperage, and volt on hardness were evaluated by analysis of variance, and the results of analysis of variance are shown in Table 9.

Table 9. ANOVA results for hardness (Sertlik için ANOVA sonuçları)

Parameters	Degrees of freedom (DoF)	Sum of squares (SS)	Mean squares (MS)	F -Value	P-Value	Percent distribution (%)
A, Welding speed (mm/min)	2	0.915440	0.457720	235.93	0.004	94.16
B, Amp (A)	2	0.029243	0.014621	7.54	0.117	3.008
C, Volt (V)	2	0.023608	0.011804	6.08	0.141	2.42
Error *(e)*	2	0.003880	0.001940			0.412
Total	8	0.972172				100

In Table 9, the analysis results of variance giving the individual effects of the experimental parameters are given. In the table, the most influential parameter affecting the hardness was welding speed with 94.16%. This parameter is followed by Ampere with 3.008%. In addition, according to the analysis of variance, the error value was minimal.

2.6. Confirmation Experiments and Taguchi Prediction Values

The purpose of validation experiments, which is the last step of the Taguchi method, is to analyze the quality characteristics. Validation experiments are also used to test the accuracy of the optimization process. In other words, validation experiments are performed to test the determined optimum combination of test parameters and levels. Considering the individual effects of the test parameters, the estimated temperature value (T_p) of $A_1B_3C_3$ (A_1= 420 mm/min welding speed, B_3 = 290 amp, C_3 = 33.6 Volt) is calculated with the equations given below, according to the optimum combination obtained for hardness [24,25].

$$\eta_{gH} = A_1 + B_3 + C_3 - 2\eta_{\frac{S}{N}-H} \quad (1)$$

$$H_p = 10^{-\eta_{gH}/20} \quad (2)$$

In equations, $A_1B_3C_3$ are the signal-to-noise ratios of the optimum levels of the experimental parameters (Table 8). $\eta_{\frac{S}{N}-H}$ is the average of the S/N ratios of the hardness values. S/N ratio calculated for η_{gH} optimum levels, H_p is the Taguchi estimate value calculated for hardness. The hardness estimation value calculated using Eq. 1 and Eq. 2 was 172.98 $HV_{0.1}$. Confidence interval (CI) compares the result of validation experiments with the predicted value and verifies the quality characteristic. The confidence interval is the maximum and minimum value, and the accuracy of the validation experiments is tested by comparing the calculated value with the predicted values. CI is calculated with the equation given below.

$$CI = \sqrt{F_{\alpha:1,Ve} x V_{ep} x \left(\frac{1}{n_{eff}} + \frac{1}{r}\right)} \quad (3)$$

In Equation 3, $F_{\alpha:1,}\nu_e$, and the significance level are the F ratio of α, α significance level, 1-α confidence interval, and the degree of freedom of the temperature error according to the variance analysis results. When Table 9 is examined, the degree of freedom of the error is 2. In this case, the 1-2 value from the F table of the 95 % confidence level was 18.5128. V_{ep} is again the error variance according to the analysis of variance results, r is the number of validation experiments, and n_{eff} is the number of effective measured results [25].

$$n_{eff} = \frac{N}{1+V_t} \quad (4)$$

In Equation 4, N represents the total number of experiments (9), and Vt represents the experimental parameters' total degrees of freedom (6). The mean is calculated by taking Table 9 into account. In this case, the n_{eff} was calculated as 1.285. In this study, considering the optimum combination determined for hardness, 3 verification tests were performed. Considering Eq. 3 and Eq. 4, the confidence interval (CI)=0.2. The Taguchi estimation value calculated for each parameter is added and subtracted with the confidence interval using the confidence interval. The mean of the validation experiments should be between these two values. The average of 3 verification tests for hardness is 173.07 $HV_{0.1}$. In this case, A range of (172.98-0.2)<173.07<(172.98+0.2)=172.78<173.07<173.18 was obtained, and confirmation experiments for hard results were performed within the confidence interval. In this case, it can be said that the optimization is successful.

Table 10 compares the experimental results with the Taguchi method's predicted values. Eq. 1 and Eq. 2 were used to calculate the estimation values. The estimated values and observed values were close to each other. Error-values should be less than 20 % for reliable statistical analysis [22].

Table 10. Comparison of optimized and random conditions with predicted values (Optimize edilmiş ve rastgele koşulların tahmin edilen değerlerle karşılaştırılması)

Levels	**Taguchi Method**		
	Experimental	**Prediction**	**Error (%)**
$A_1B_3C_3$ (Optimum)	173.07	172.98	0.05
$A_2B_1C_2$ (Random)	183.20	182.81	0.21
$A_1B_3C_3$ (Random)	173.40	172.98	0.24
$A_3B_1C_3$ (Random)	191.70	191.86	0.08
$A_3B_3C_2$ (Random)	189.70	190.33	0.33

In Table 10, experimental results and Taguchi prediction values are compared. It is seen that the error values between the confirmation test results and the results obtained by the Taguchi method

are less than 20 % or even minimal. In this case, the results obtained from the validation experiments show that the optimization has been carried out successfully.

3. EXPERIMENT AND OPTIMIZATION RESULTS (DENEY VE OPTİMİZASYON SONUÇLARI)

3.1.The finite element analysis result

Finite element analysis was performed based on sample no. 3 (420 mm/min welding speed, 290 Amps, and 33.6 Volts), the lowest hardness value was reached due to Taguchi optimization and verification experiments. It is thought that the finite element analysis performed by obtaining the lowest hardness value will be a reference among other results. The change in the macrostructure resulting from the finite elements made is compared with the accurate macro structure results in Figure 4. When Figure 4 is examined, it is seen that the macrostructure image formed after the welding process and the estimated macro structure image formed by the finite element analysis are close to each other. As a result, the estimated finite element method is considered successful.

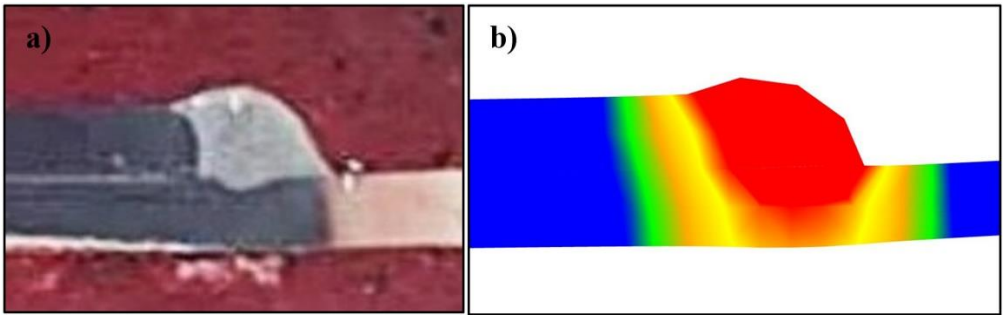

Figure 4. The finite element analysis comparison; a) Welding macrostructure, b) The finite element analysis macrostructure (Sonlu elemanlar analizi karşılaştırması; a) Kaynak makro yapısı, b) Sonlu elemanlar analizi makro yapısı)

The finite element analysis results of heat exchange and distortion rates during welding are given in Figures 5 and 6. When Figure 5 is examined, the values at which the heat generated during welding reaches the highest temperature are shown.

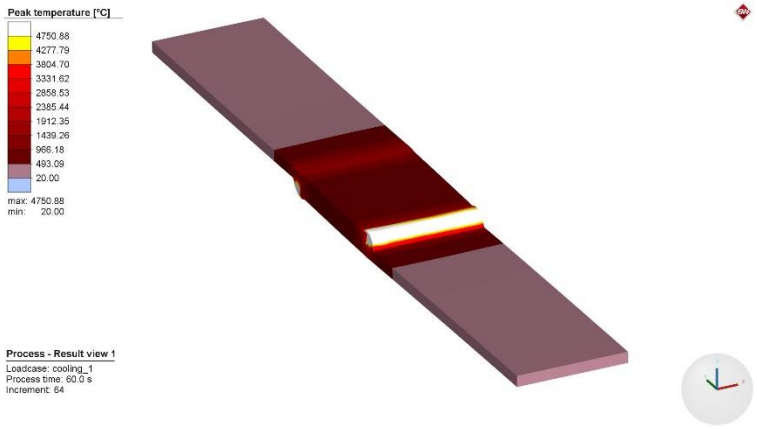

Figure 5. MAG welding temperature peak values (MAG kaynak sıcaklığı tepe değerleri)

In Figure 6, the maximum temperature reached during welding, and the maximum amounts of deformation after welding are given. It is predicted that the maximum amount of deformation after the welding process estimated with finite elements will be 1 mm. As a result of the measurements made after the welding process, the total amount of deformation in the natural welded joint was measured as 1.6 mm. This value is considered close to the weight estimated by the finite element software.

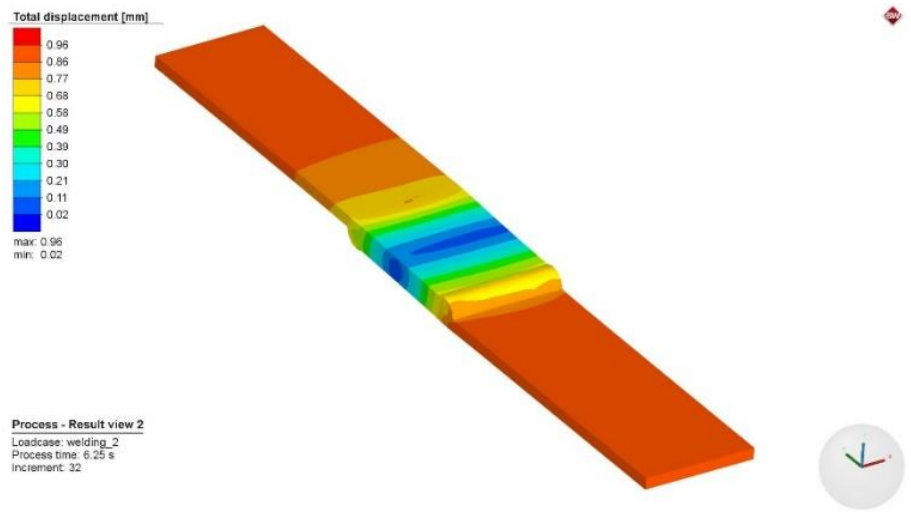

Figure 6. The amount of deformation after welding (Kaynak sonrası deformasyon miktarı)

3.2. A mathematical model with regression method model

This study determined the correlation level between hardness values and experimental parameters using the polynomial regression model. Multiple regression analysis can derive estimation equations of continuous dependent variables obtained through experimental designs with each combination of control factors. The equation (Eq. 5) predicted for the quadratic regression model is shown below:

$$H_r = 73 - 0.0159\ Vw + 1.37\ A - 4.30\ V + 0,.000038\ Vw^2 - 0.00267\ A^2 + 0.0622\ V^2 \quad (5)$$

H_r represents the estimation equation for the hardness values using the test parameters. According to the regression results, the R^2 value of the obtained mathematical model was calculated as 0.995 (99.5%).

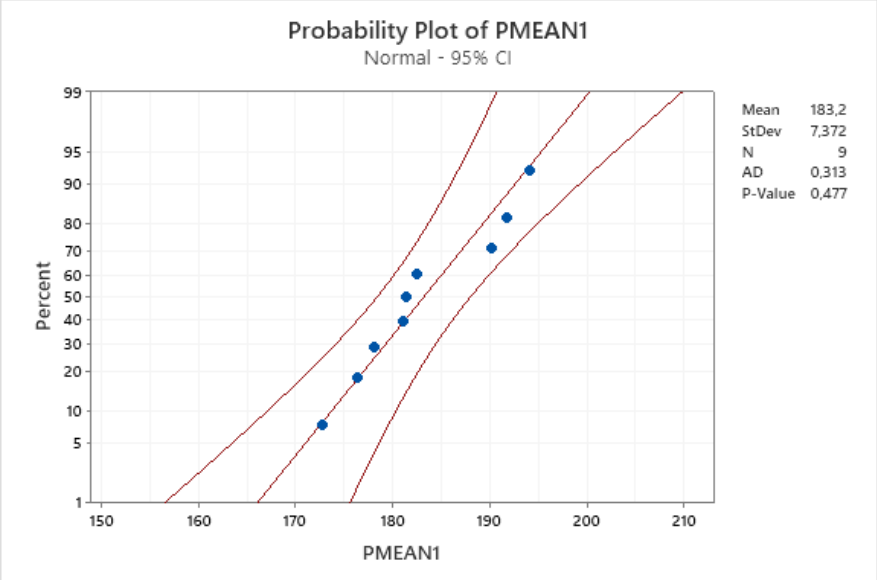

Figure 7. Probability plot (Olasılık grafiği)

The probability plot is given in Figure 7. The figure shows that the prediction values are within the 95 % confidence interval. As a result, it is thought that the estimated values will give results close to the truth.

3.3. Effects of test parameters on hardness

The effects of test parameters on hardness were examined with three-dimensional graphics (Figure 8).

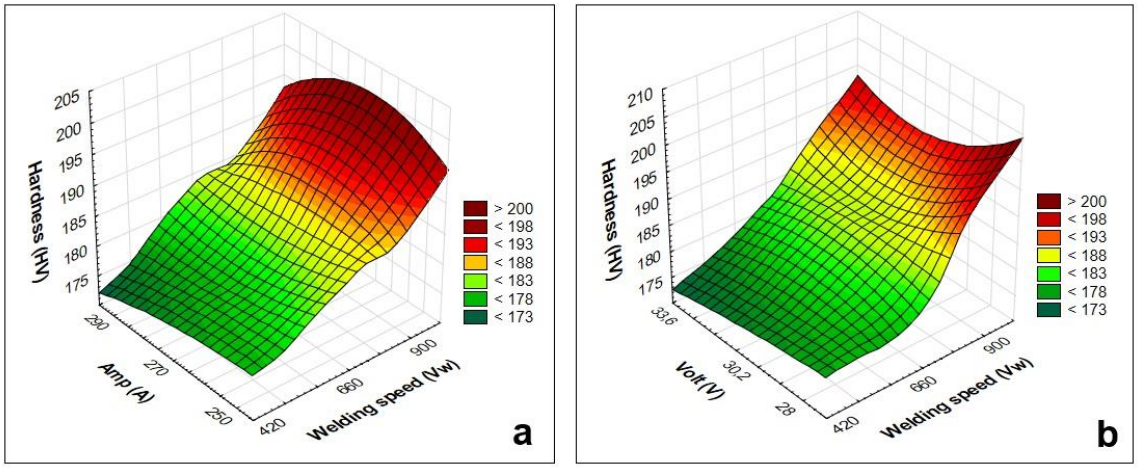

Figure 8. Effect of test parameters on hardness (Test parametrelerinin sertlik üzerindeki etkisi)

In Figure 8a, the effect of amperage and welding speed on hardness is given with a three-dimensional graphic. Here, it is seen that the hardness increases as the welding speed increases. In Figure 8a, it is seen that the best result is 420 mm/min welding speed and 290 A amperes. This result is similar to Taguchi's optimized values. In Figure 8b, a three-dimensional graph showing the effect of volt and welding speed on hardness [26]. Here, it is seen that the hardness increases as the welding speed increases. Figure 8b shows the best results at 33.6 Volts and 420 mm/min welding speed. This situation is similar to Taguchi's optimized values.

4. CONCLUSIONS (SONUÇLAR)

In this study, Taguchi optimization and finite element analysis of the lap welding of DD13 sheets used in the manufacture of automobile swing arms were performed. The data obtained as a result of experimental studies are listed below.

- It has been observed that DD13 sheets are joined together without any problems with the MAG welding method.
- This study successfully applied Taguchi optimization with a 95 % confidence interval. The R^2 value of the mathematical model obtained according to the regression results was calculated as 0.0995.
- As a result of the optimization process, it has been determined that the welding speed is the effective parameter with 94.16 % of the hardness in the weld seam. This parameter is followed by welding amperage with 3.008 % and welding voltage with 2.83 %.
- As a result of Taguchi optimization, the lowest hardness value was estimated as 172.98 $HV_{0.1}$ in MAG welding performed with 420 min/mm welding speed, 290 A, and 33.6 V parameters. The validation test result was found to be consistent with 173.4 $HV_{0.1}$.
- It was observed that the error between the validation experiments and the prediction values obtained by the Taguchi method was less than 20%. In this case, the results obtained with the validation experiments show that the optimization process has been carried out successfully.
- Finite element analysis has been successfully applied in this study. It has been seen that the estimated macro structure image and the natural source macro structure image are close to each other.
- As a result of the analysis, the estimated distortion value obtained after the welding process was seen as approximately 1 mm, while the actual distortion value was measured as 1.6 mm.

ACKNOWLEDGMENTS (TEŞEKKÜR)

Thanks to NETFORM Engineering Machinery Metal Ltd. for their support in the finite element analysis of this study.

REFERENCES (KAYNAKLAR)

1. L. Tang, J. Wu, J. Liu, C. Jiang, W.-B. Shangguan, Topology optimisation and performance calculation for control arms of a suspension, Advances in Mechanical Engineering, 6:1-10, 2014.
2. H.B. Zhang, R.J. Zhang, Y. Chang, Finite element analysis of automobile suspension control arm, Applied Mechanics and Materials, 752–753: 859–863, 2015.
3. H.B. Zhang, Y. Chang, R.J. Zhang, H.Y. Fan, Reverse modeling of vehicle suspension control arm, Applied Mechanics and Materials, 427–429: 1183–1186, 2013.
4. B.K. N, Design and analysis of sheet metal control arm, International Journal of Science and Research, 4 (11): 1241–1248, 2015.
5. James D. Halderman, Automotive Steering, Suspension & Alignment, 5. Edition, Pearson, New Jersey, 2010.
6. M. Bouazara, Improvement in the Design of Automobile Upper Suspension Control Arms Using Aluminum Alloys, Damage Fract. Mech., Springer Netherlands, Dordrecht, 101–112, 2009.
7. M. Shome, M. Tumuluru, Introduction to welding and joining of advanced high-strength steels (AHSS), in: M. Shome, M.B.T.-W. and J. of A.H.S.S. (AHSS) Tumuluru (Eds.), Woodhead Publishing, 1-8, 2015.
8. M.A. Wahab, Manual Metal Arc Welding and Gas Metal Arc Welding, in: S. Hashmi, G.F. Batalha, C.J. Van Tyne, B.B.T.-C.M.P. Yilbas (Eds.), Elsevier, Oxford, 49-76, 2014.
9. Z. Boumerzoug, C. Derfouf, T. Baudin, Effect of welding on microstructure and mechanical properties of an ındustrial low carbon steel, Engineering, 02: 502-506, 2010.
10. P. Kah, R. Suoranta, J. Martikainen, Advanced gas metal arc welding processes, The International Journal of Advanced Manufacturing Technology, 67: 655-674, 2013.
11. J. Frei, B.T. Alexandrov, M. Rethmeier, Low heat input gas metal arc welding for dissimilar metal weld overlays part I: the heat-affected zone, Welding in the World, 60: 459-473, 2016.
12. V. Tandon, M.A. Thombre, A.P. Patil, R. V. Taiwade, H. Vashishtha, Effect of heat ınput on the microstructural, mechanical, and corrosion properties of dissimilar weldment of conventional austenitic stainless steel and low-nickel stainless steel, Metallography, Microstructure, and Analysis, 9: 668-677, 2020.
13. S. Madhavan, M. Kamaraj, B. Arivazhagan, A comparative study on the microstructure and mechanical properties of fusion welded 9 Cr-1 Mo steel, J. Mater. Res. Technol., 9: 2223-2229, 2020.
14. U. Çaligülü, H. Dikbaş, M. Taşkin, Microstructural characteristic of dissimilar welded components (AISI 430 ferritic-AISI 304 austenitic stainless steels) by CO2 laser beam welding (LBW), Gazi University Journal of Science, 25: 35-52, 2012.
15. S. Selvi, A. Vishvaksenan, E. Rajasekar, Cold metal transfer (CMT) technology - An overview, Defence Technology, 14: 28-44, 2018.
16. R. Talalaev, R. Veinthal, A. Laansoo, M. Sarkans, Cold metal transfer (CMT) welding of thin sheet metal products, Est. J. Eng., 18: 243, 2012.
17. M. Grzybicki, J. Jakubowski, Comparative tests of steel car body sheet welds made using CMT and MIG/MAG methods, Welding International, 27: 610-615, 2013.
18. M. Korzeniowski, T. Piwowarczyk, P. Kustroń, A. Czubak, Low-energy welding methods used for semi-automatic thin-walled automotive steels, Advances in Materials Science, 13(3): 2013.
19. Y. Liu, L. Zhang, Y. Chen, Application of Cold Metal Transition Technology in Automobile Manufacture, in: Proc. 2018 7th Int. Conf. Energy, Environ. Sustain. Dev. (ICEESD 2018), Atlantis Press, Paris, France, 1170-1173, 2018.
20. J. Subramanian, S. Ganguly, W. Suder, D. Mukherjee, Investigation of functional and aesthetic quality of weld for different arc modes in CMT, Int. Res. J. Eng. Technol., 07: 4497-4502, 2020.
21. B. Chen, W. Xiao, L. Zhu, F. Zhang, Analysis on the Microstructure and Mechanical Properties of Welding Joint of Low Alloy Structural Steel Plate by Narrow Gap MAG, Proc. Int. Conf. Mechatronics, Electron. Ind. Control Eng., Atlantis Press, Paris, France, 2015.
22. G. Samtaş, S. Korucu, Multiple optimisation of cutting parameters in milling of cryogenically treated Aluminium 6061-T651 alloy with cryogenic and normal cutting inserts, Surface Topography: Metrology and Properties, 9: 2021.
23. H.R. Ghanbari, M. Shariati, E. Sanati, R. Masoudi Nejad, Effects of spot welded parameters on fatigue behavior of ferrite-martensite dual-phase steel and hybrid joints, Eng. Fail. Anal., 134: 106079, 2022.
24. A.K. Pattanaik, S.N. Panda, K. Pal, D. Mishra, A comparative investigation to process parameter optimization for spot welding using Taguchi based grey relational analysis and metaheuristics, Mater. Today Proc., 11408–11414, 2018.

25. G. Samtaş, Optimisation of cutting parameters during the face milling of AA5083-H111 with coated and uncoated inserts using Taguchi method, International Journal of Machining and Machinability of Materials, 17: 211–232, 2015.
26. V. Onar, Robotik MAG kaynak metodunda XAR 500 serisi çeliklerin mikrosertliğine farklı kaynak akımlarının ve hızlarının etkisi, Düzce Üniversitesi Bilim ve Teknoloji Dergisi, 8(1): 1193-1203, 2020.